Effect of alloying addition of Pr on the dissolution rate of melt-spun Mg in 3% NaCl solution

Y. LI, J. LIN*, F. C. LOH*, K. L. TAN*, G. L. CHEN*, C. H. KAM
*Departments of Materials Science and *Physics, National University of Singapore, Singapore 119260*

Melt-spun Mg-1 and 15 wt % Pr binary alloys were immersed in a 3% NaCl solution saturated with $Mg(OH)_2$ for up to 72 h. The dissolution rate was evaluated by hydrogen evolution method. Surface characterization of the pristine and corroded surfaces has been carried out using X-ray photoelectron spectroscopy (XPS), secondary ion mass spectroscopy (SIMS), X-ray diffraction (XRD) and scanning electron microscopy (SEM). The surfaces of both the pristine and corroded samples were found to consist mainly of $Mg(OH)_2$ and MgO. However, results of XRD and SEM showed that the dominant product formed on the corroded sample was $Mg(OH)_2$. SIMS depth profiling showed that there was a depletion of Pr at the surfaces of Mg–Pr samples. © *1998 Chapman & Hall*

1. Introduction

In general, magnesium alloys produced by conventional ingot metallurgy processing exhibit poor corrosion resistance. The application of rapid solidification (RS) processing can result in the refinement of both matrix grains and intermetallic particles, extension of solid solubility, formation of non-equilibrium phases (including crystalline, quasicrystalline and non-crystalline) and improved chemical homogeneity. RS processing of appropriate magnesium alloys can improve their corrosion resistance by contributing towards the formation of protective films and the elimination of microgalvanic effects. As a result, a number of workers have studied the effects of RS processing and alloy elements on the corrosion resistance of Mg-based alloys, with emphasis on the effects of added Al and rare earths [1–3]. Rugg *et al.* [1] reported that the introduction of 1 wt % Nd as a ternary addition gives a further reduction in dissolution rate in 3 % NaCl for splat quenched Mg–4.7 wt % Mn alloy after immersion for 50 h. Das *et al.* [2–3] reported that Nd-containing EA55RS (Mg–5 wt % Al–5 wt % Zn–5 wt % Nd) extrusion gave a dissolution rate in 3% NaCl of 279 μm/year compared with 1.27 mm/year for Nd-free AZ91 HP-T6.

The present paper reports our results of the effects of Pr additions on the dissolution rate of rapidly solidified magnesium in 3% NaCl solution saturated with $Mg(OH)_2$ and the characterization of corroded products formed on the surface of these samples.

2. Experimental procedure

Details of alloy preparation and melt-spinning of Mg–Pr binary alloys have been reported previously [4]. A 3% NaCl solution saturated with magnesium hydroxide was used for the corrosion test [1]. These tests were carried out in a glass container containing the solution at $25 \pm 0.1\,°C$ for 5 min to 72 h. The corrosion test involved measuring the rate of accumulation of hydrogen evolved by the corroding sample in a calibrated hydrogen collection glass tube [1]. After the corrosion test, the specimens were briefly washed with water and acetone and drained of excess solution on to a tissue paper, and finally air dried. X-ray photoelectron spectroscopy (XPS) experiments were carried out in a VG Escalab MKII spectrometer at a constant analyser pass energy of 20 eV. MgK_α X-ray (1253.6 eV photon, 120 W) was used as the excitation source. The secondary ion mass spectroscopy (SIMS) experiments were performed in a VG SIMSLAB system. Both the XPS and SIMS chambers were connected via a preparation chamber, the normal operating pressure in all chambers being $< 2 \times 10^{-7}$ Pa during the course of the experiments. The primary ion source of SIMS was a 9 keV, 100 nA Ar beam, which was incident on the sample surface at 45° in the reduced area mode. X-ray diffraction was performed in a Philips 1700 diffractometer with CuK_α radiation and scanning electron microscope (SEM) studies were carried out in a Jeol 50 electron microscope.

3. Results
3.1. Results of corrosion test
Fig. 1 shows the effect of 1 wt % Pr and 15 wt % Pr additions on the dissolution rate of magnesium as-spun, displaying continuous decrease rate with duration of the immersion up to 72 h. It also shows that the dissolution rate of as-spun Mg–1 wt % Pr ribbons is much lower than that of as-spun Mg–15 wt % Pr ribbons, although both rates are much lower than that of melt-spun pure magnesium ribbons [5].
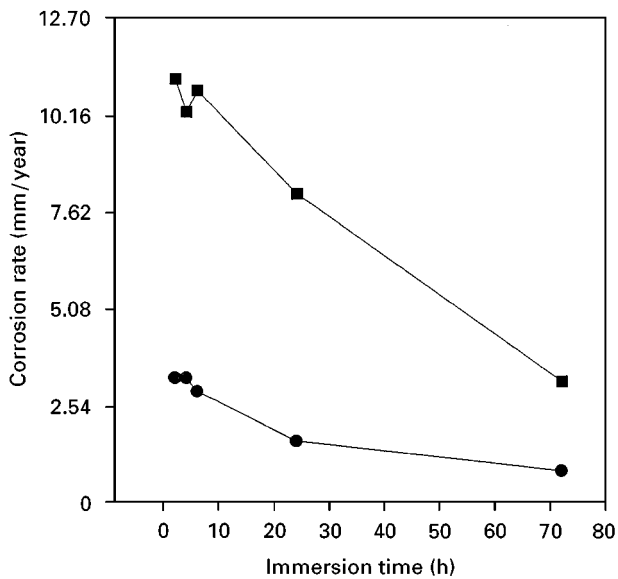
Figure 1 Dissolution rate via hydrogen evolution testing as a function of time in 3% NaCl solution for melt-spun Mg–1 wt % Pr (●) and Mg–15 wt % Pr (■) alloys.

3.2. Results of SEM and X-ray diffraction (XRD)

Fig. 2 shows the surface morphology of free and chill sides of as-spun Mg–15 wt % Pr ribbon. On the free side, the occurrence of inhomogeneous regions mainly consisting of "hills" and "valleys" was observed. On the chill side a dendritic morphology together with air
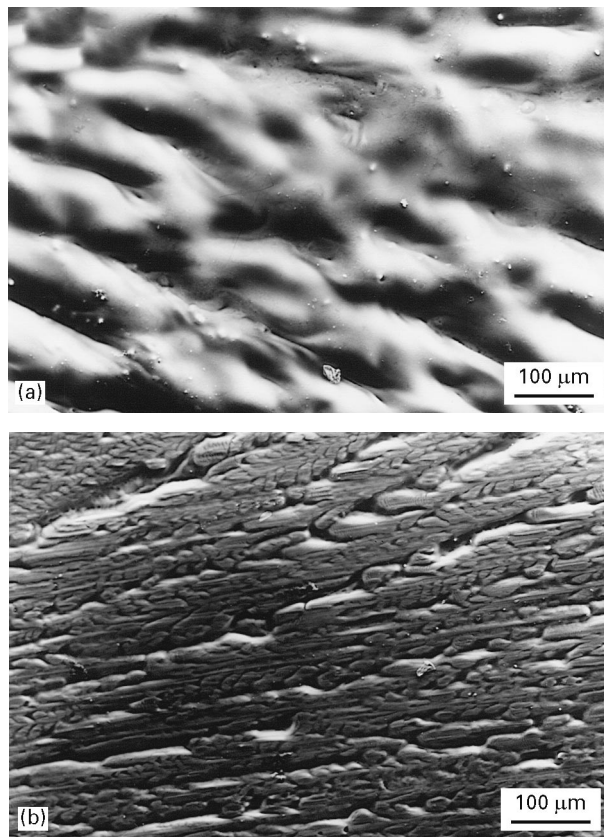
Figure 2 Surface morphology of as-spun Mg–15 wt % Pr ribbon: (a) free side and (b) chill side.
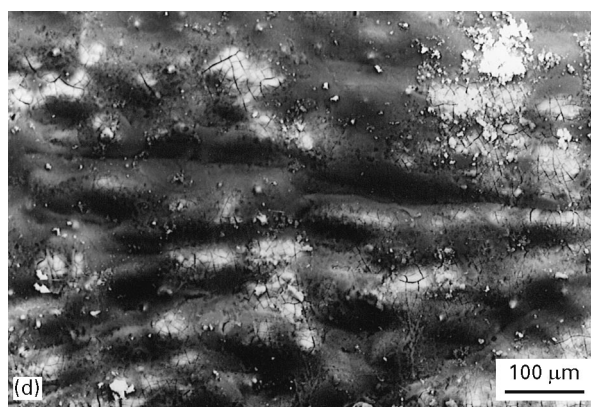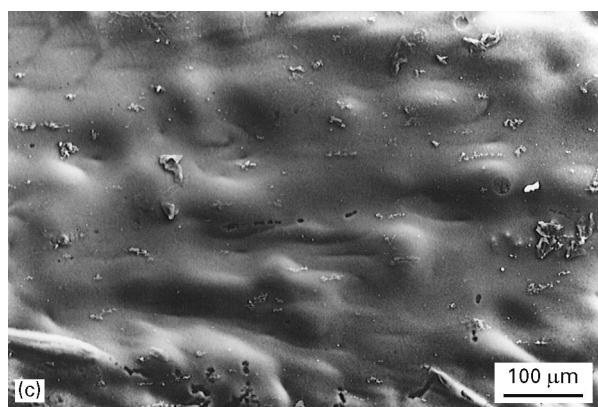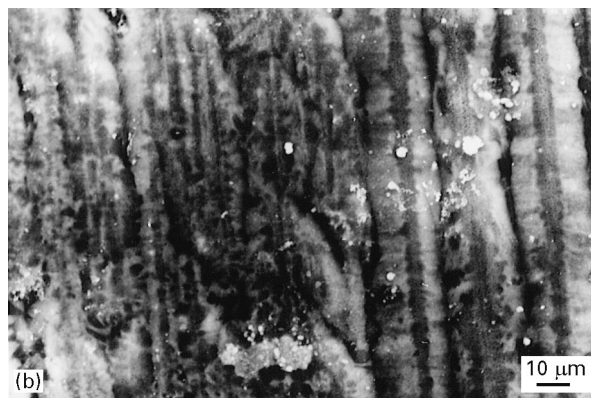
Figure 3 SEM micrographs showing the chill surfaces of (a) Mg–1 wt % Pr and (b) Mg–15 wt % Pr ribbons after immersion in 3% NaCl solution for 20 h: SEM micrographs showing the free surface of (c) Mg–1 wt % Pr and (d) Mg–15 wt % Pr ribbons after immersion in 3% NaCl solution for 10 h.

1076
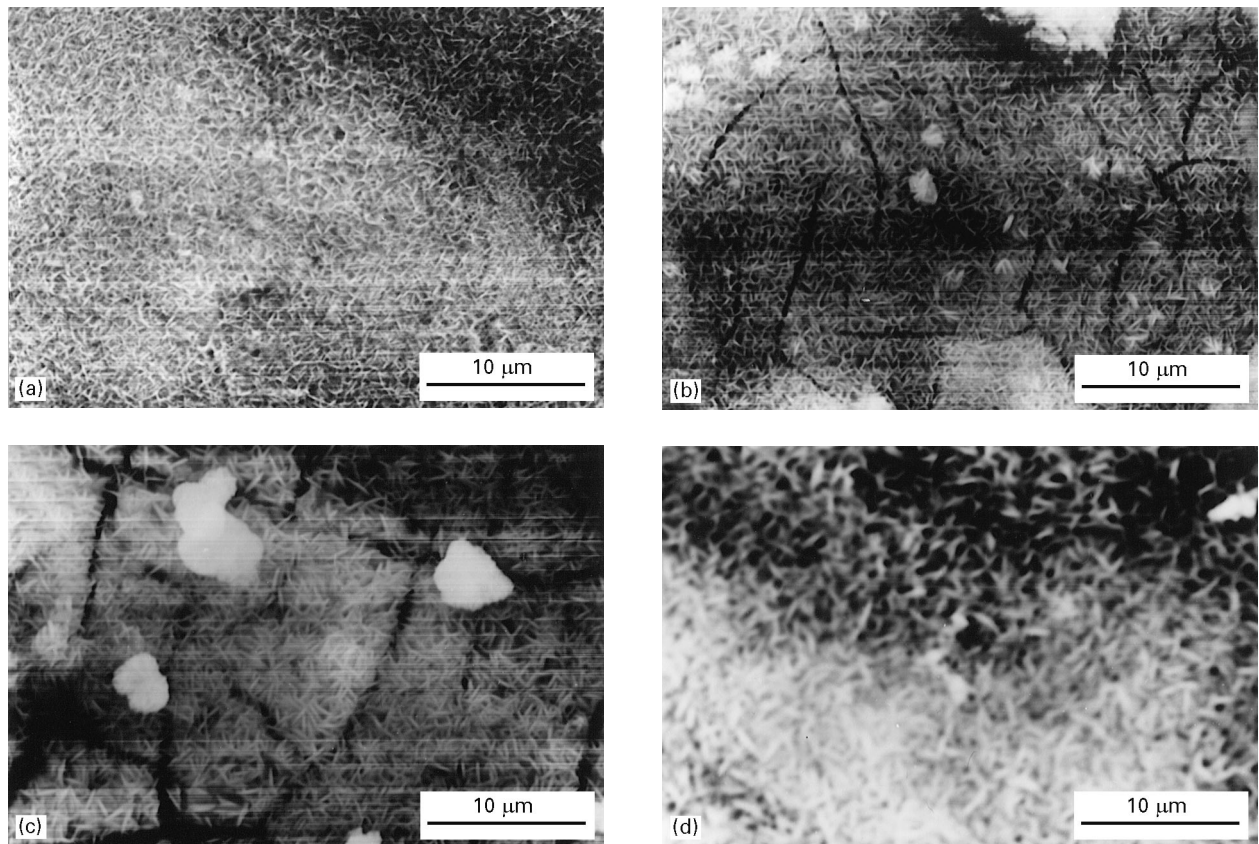
Figure 4 SEM micrographs at higher magnification showing the voluminous fine needle-like acicular structure formed on the Mg–15 wt % Pr free surfaces of (a) 20 min, (b) 2 h, (c) 5.25 h and (d) 20 h immersion in 3% NaCl solution, respectively.

bubbles can be clearly seen. Ribbons of Mg–1 wt % Pr exhibited similar morphology to that of free and chill sides of Mg–15 wt % Pr ribbons. Fig. 3a–d shows that after immersion in 3% NaCl solution, there was less corrosion product formed on the surface of Mg–1 wt % Pr (Fig. 3c) than on Mg–15 wt % Pr ribbons (Fig. 3d), which is consistent with the corrosion test results that the corrosion resistance of Mg–1 wt % Pr was better than that of Mg–15 wt % Pr ribbons. Higher magnification of the Mg–15 wt % Pr sample after corrosion showed needle-like structures and the continuous coarsening of such needles (Fig. 4). The X-ray diffraction results for melt-spun Mg–1 wt % Pr in Fig. 5 show that while only αMg was present in the pristine sample, Mg(OH)$_2$ appeared on the sample after immersion, corresponding to the needle-like materials shown in Fig. 4.

3.3. Results of XPS

Fig. 6a–d show O 1s and Mg 1s core-level spectra of the Mg–1 wt % Pr sample after immersion in 3% NaCl solution for different lengths of time. These show that the predominant species on the surface of the pristine Mg–1 wt % Pr sample was MgO, while after immersion for 20 h in 3% NaCl solution, the predominant species on the surface of Mg–1 wt % Pr was magnesium hydroxide. Fig. 7a–d shows O 1s and Mg 1s core-level spectra of Mg–15 wt % Pr sample after immersion in 3% NaCl solution for different lengths of time. These show that the predominant species on the surface of the pristine Mg–15 wt % Pr sample was
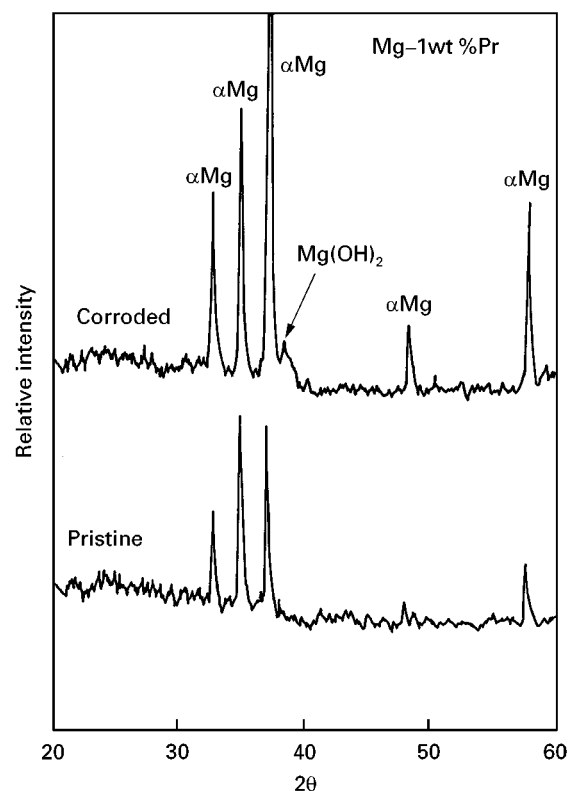
Figure 5 XRD results for Mg–1 wt % Pr sample after immersion in 3% NaCl solution for different lengths of time showing only Mg and Mg(OH)$_2$ present on the sample surface.

Mg(OH)$_2$ together with a large amount of MgO, while the amount of MgO has been reduced on the surface of the sample after immersion for 5.25 h in 3% NaCl
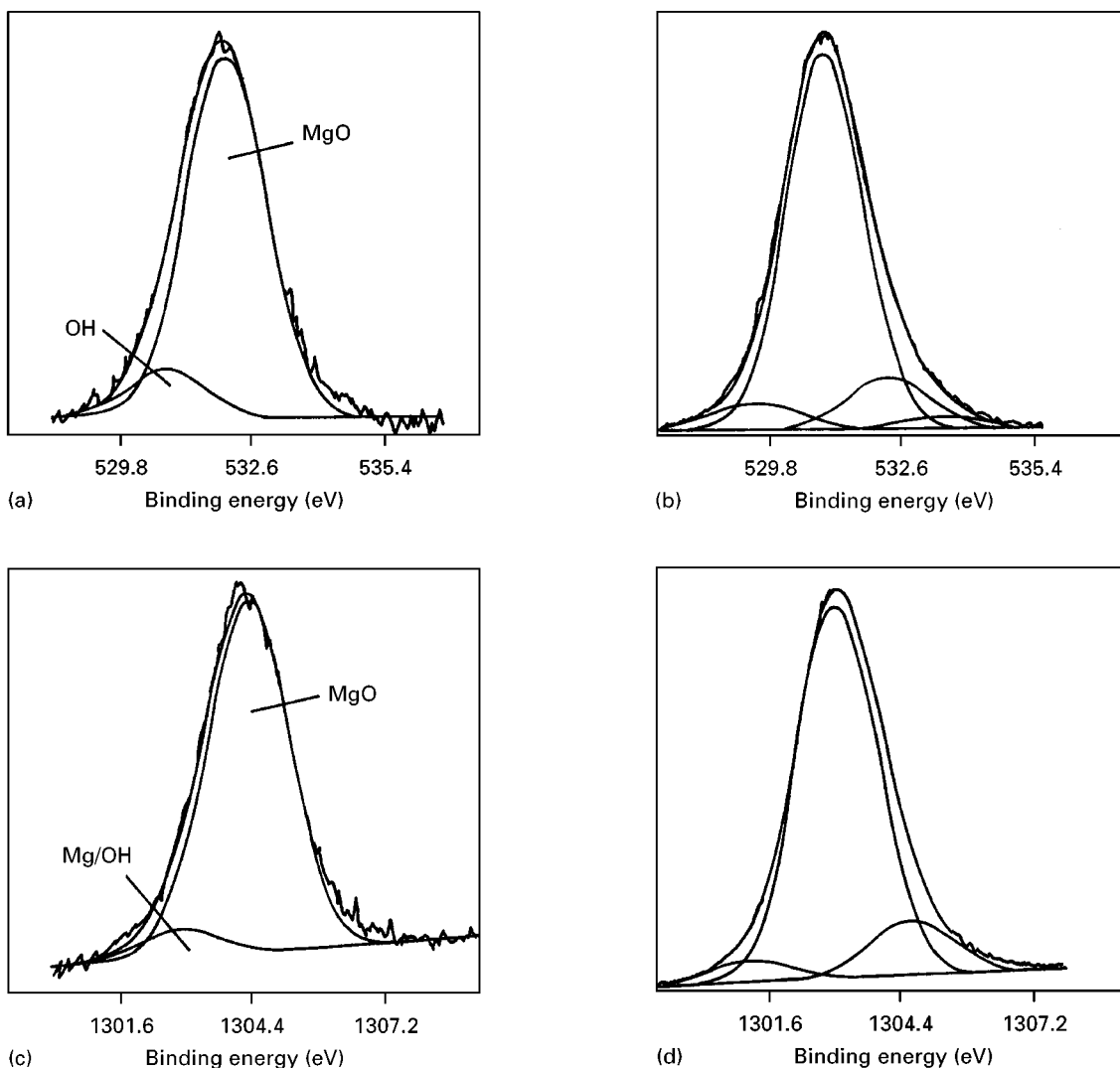
Figure 6 O1s (a and b) and Mg1s (c and d) core-level spectra of Mg–1 wt % Pr sample after immersion in 3% NaCl solution for difference lengths of time: (a and c) pristine sample and (b and d) after 20 h.

solution. XPS results for all the samples studied indicate that $Mg(OH)_2$ and MgO were found on the surfaces of pristine and corroded samples with $Mg(OH)_2$ as the predominant species after long immersion times.

Fig. 8a shows the Pr 3d core-level spectrum of pristine Mg–15 wt % Pr ribbon as-spun. The broad peak may be decomposed into four peaks at binding energy 929.15, 931.75, 933.20 and 934.75 eV according to peak synthesis results. On the basis of known data [6], the peak at 931.75 eV arises from metallic Pr while the one at 933.2 eV from Pr in Pr_2O_3. No data have been reported for the peaks at other positions. In the present case, the other peaks observed may be attributed to monovalent Pr^+ species at 929.15 eV and Pr in its corresponding hydroxide $Pr(OH)_3$ species at 934.75 eV. Attribution of the later species has been supported by the presence of Pr–OH in the SIMS data. Curve fitting of the broad peak for the corroded sample (Fig. 8b) reveals similar peak assignments as those of the pristine sample, with the only difference being the relative low intensities, indicating the reducing amount of Pr-related species on the sample surface.

3.4. Results of SIMS

The results of SIMS depth profiling of Mg–15 wt % Pr ribbons are given in Fig. 9a, b for the pristine surface and the surface of the sample immersed in solution for 5.25 h. For the pristine sample, the relative intensities of Mg and Pr secondary ions in the surface region remain almost the same as in the bulk, although they are all enhanced probably as a result of the presence of oxygen on the surface. Pr–O species is also found to be more predominant in the surface region than metallic Pr, while Pr–OH species is the least abundant. For the immersed sample, it is noticed that Pr showed trends of depletion in the surface region. This is obvious as the Pr–OH species then exhibits similar intensity to Pr while the intensity of Mg–OH species has increased, relatively, with respect to Pr compared to the pristine sample.

Fig. 10a displays the positive secondary ion mass spectrum for the pristine sample, indicating that the main species on the surface are H, Mg (whose isotopic abundances are 24 a.m.u., 79%; 25 a.m.u., 10%; 26 a.m.u., 11%), MgO (40 a.m.u.), Mg–OH (41, 42, 43 a.m.u.), Pr (141 a.m.u.), Pr–O (157 a.m.u.) and Pr–OH (158 a.m.u.). The spectrum (Fig. 10b) of the
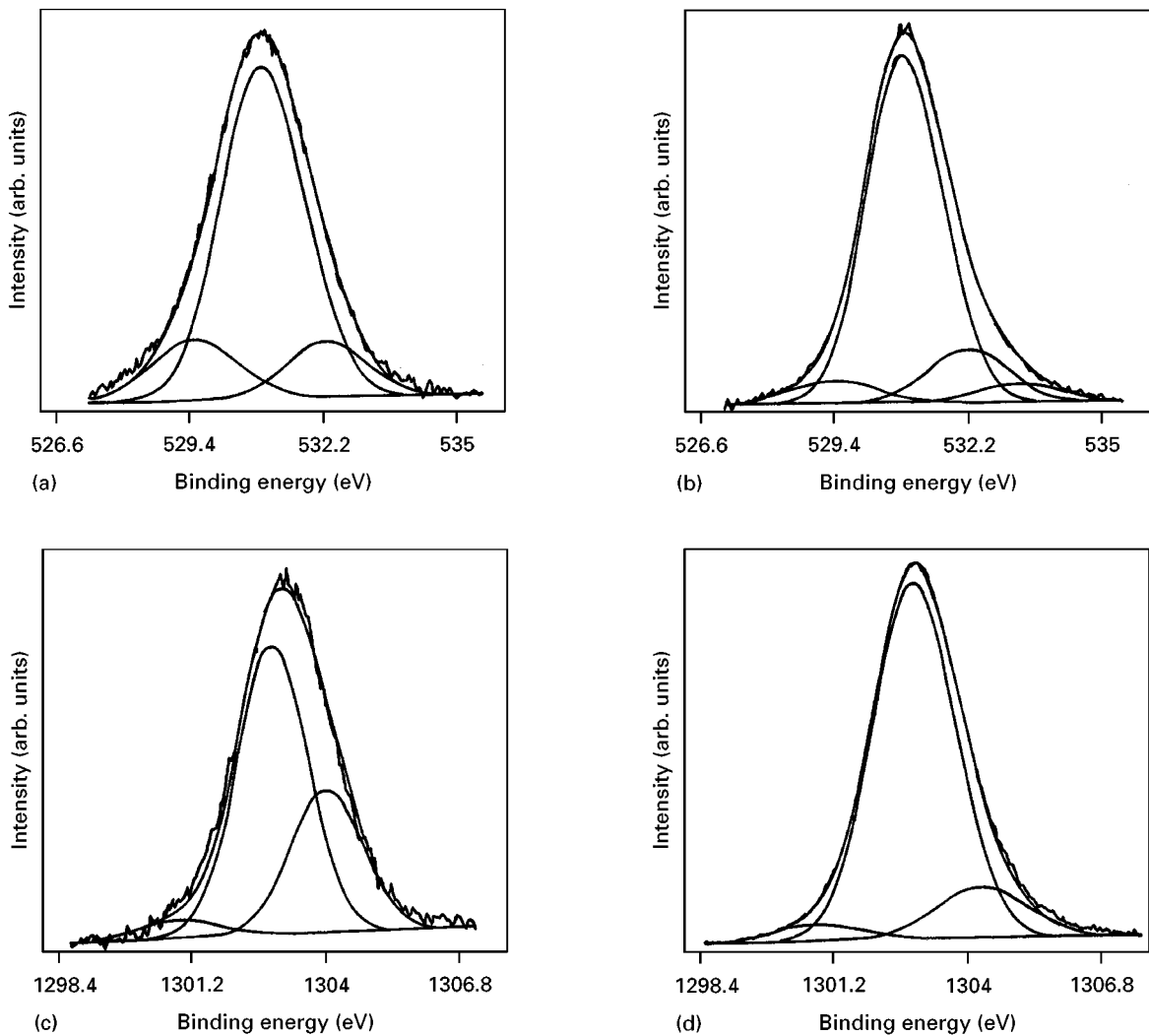
Figure 7 O1s (a and b) and Mg1s (c and d) XPS core-level spectra of Mg–15 wt % Pr sample after immersion in 3% NaCl solution for different lengths of time: (a and c) pristine sample and (b and d) after 5.25 h.
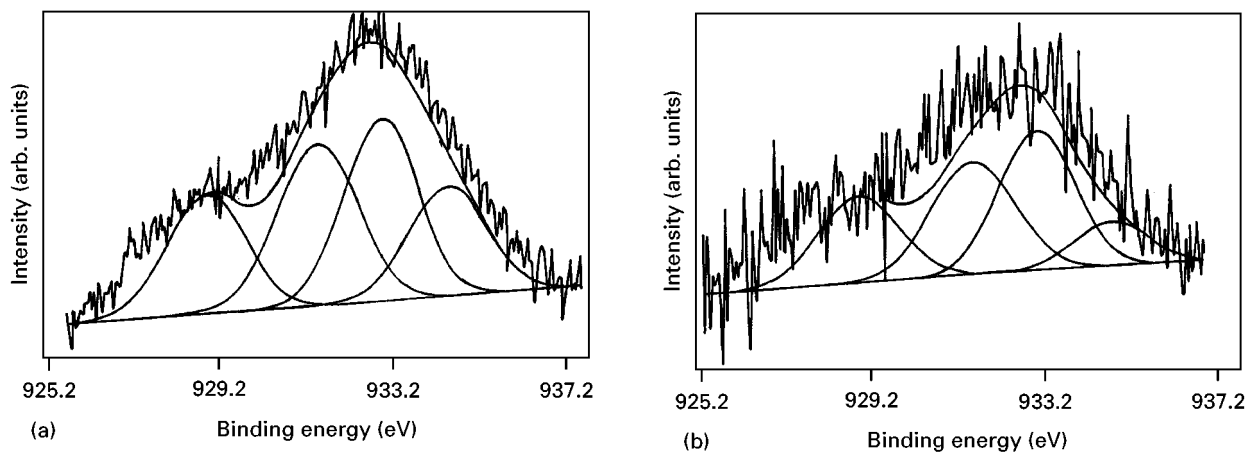
Figure 8 Pr 3d XPS core-level spectra of Mg–15 wt % Pr sample after immersion in 3% NaCl solution for different lengths of time: (a) pristine sample and (b) after 5.25 h.

sample after immersion of 5.25 h is similar to that of the pristine sample with dominant surface species of H, Mg, MgO, Mg–OH, Pr, Pr–O and Pr–OH. The hydrogen peak at 1 a.m.u. and the Mg–OH peak at 41–43 a.m.u. are relatively more intense in the positive SIMS mass spectrum after immersion.

4. Discussion

Fig. 1 shows that the effect of rare earth Pr additions in Mg gives rise to a dissolution rate that decreases continually with increased duration of immersion. This result is consistent with previous reports on the effects of Nd and Y on the dissolution rates of splat
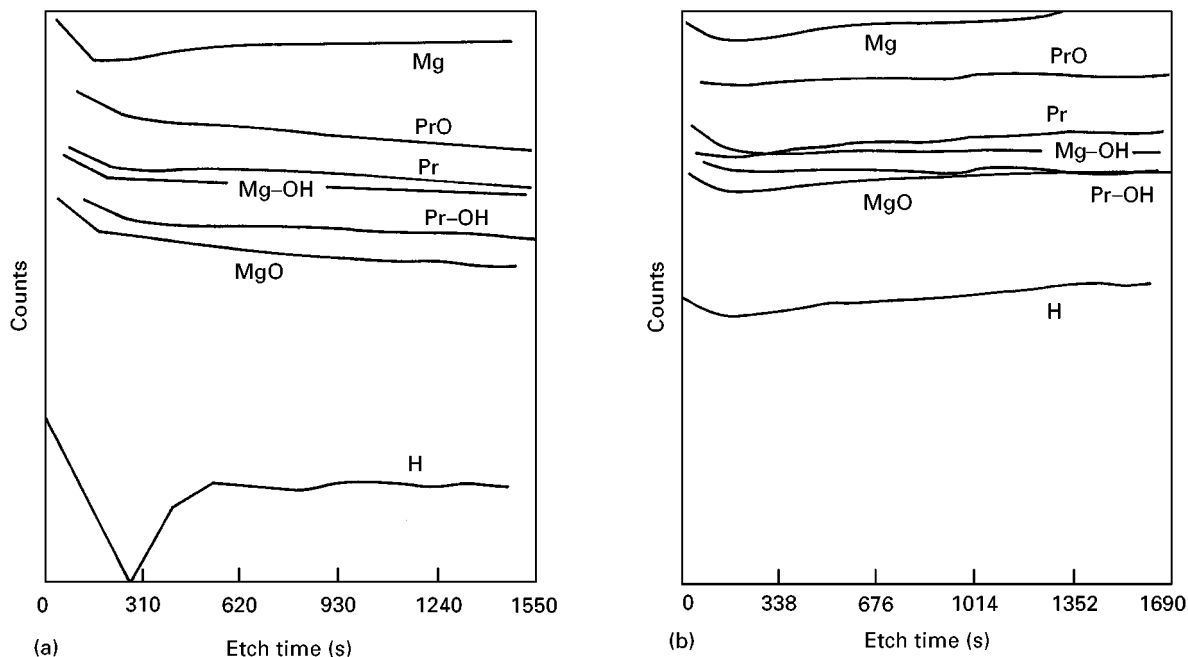
Figure 9 Results of SIMS positive depth profiling of Mg–15 wt % Pr sample after immersion in 3% NaCl for different lengths of time: (a) pristine sample and (b) 5.25 h, showing the depletion of Pr for corroded sample surface.
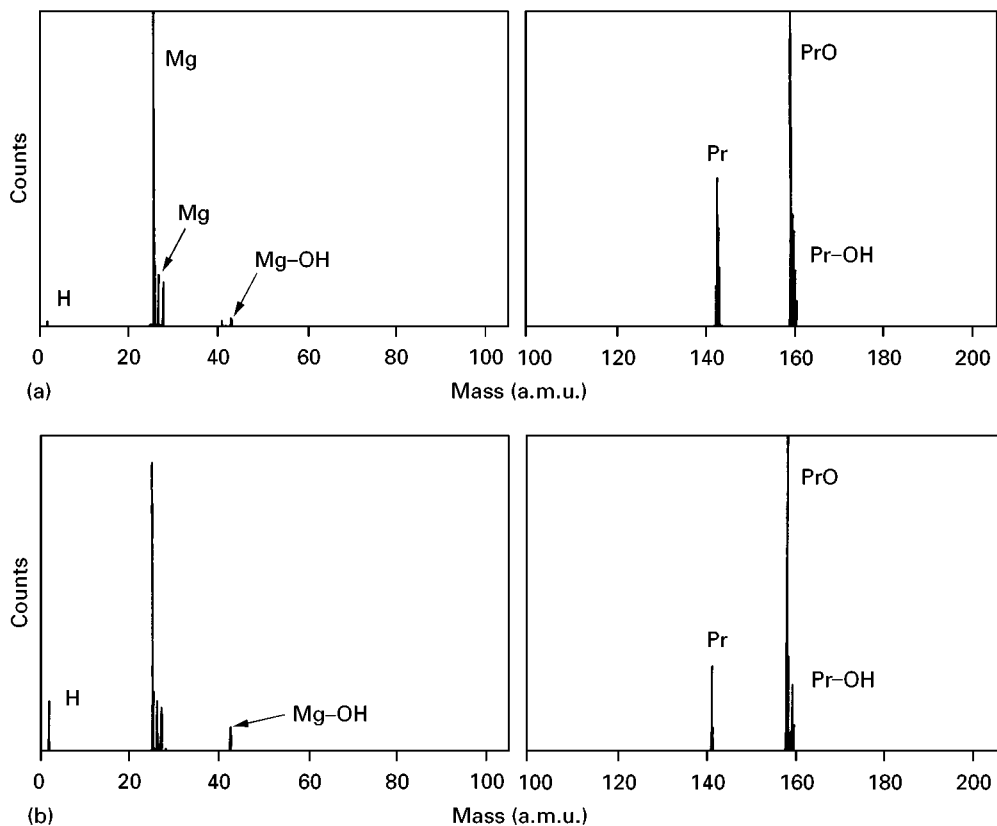
Figure 10 Positive secondary ion mass spectra of Mg–15 wt % Pr sample after immersion in 3% NaCl solution for different lengths of time: (a) pristine sample and (b) 5.25 h, showing the increment of H and Mg–OH species.

quenched Mg–Mn alloys and in contrast with the effect of Ni, Cu and Si [1]. The dissolution rate as a function of time for melt-spun Mg–15 wt % Pr is higher than that of Mg–Mn–Nd reported before, while the dissolution rate of Mg–1 wt % Pr is highly comparable with those of Mg–Mn–Nd alloys in which the range of Nd content was from 0.2 to 1 wt % [1]. Present results clearly indicate that there is an optimal concentration of rare elements on the reducing dissolution rates of magnesium in 3% NaCl solution. Our previous transmission electron microscopy (TEM) microstructural investigation [4] of Mg–1 wt % Pr and Mg–15 wt % Pr revealed that there were equiaxed Mg grains with few dispersive second phase along-grain boundaries, whereas primary Mg with some Mg–Pr secondary phases plus

degenerated lamellar eutectic formed in Mg–15 wt % Pr as-spun samples. Pr-rich particles may act as the corrosion nucleation sites and this should explain why the melt-spun Mg–1 wt % Pr has a lower dissolution rate than that of melt-spun Mg–15 wt % Pr.

Krishnamurthy *et al.* reported [8] that pseudopassivation occurred in rapidly solidified Mg–Nd and Mg–Y alloys and they related this occurrence to be a result of more homogeneous and refined microstructure produced by RS processing. This was accompanied by a moderate enrichment of the surface in Nd. Das *et al.* [3] attributed the improvement of corrosion resistance by Nd to Mg-based alloys to a protective or semiprotective film on the surface of the sample as a result of a reaction of the saline solution with Nd. From the present study, it was found that $Mg(OH)_2$ was still the dominant corrosion product for Mg–Pr ribbons after immersion. Our previous report [7] on the surface characterization of EA55RS (Mg–5 wt % Al–5 wt % Zn–5 wt % Nd) extrusion showed that no Nd was detected in the surface region (i.e. within 10 nm of the surface) for either pristine or corroded samples by XPS and there was a depletion of Nd on the surface of the corroded sample for the depth of 0.4 to 2 μm by SIMS. Our present results of SIMS depth profiling (Fig. 9) on corroded melt-spun Mg–Pr alloys, as well as the results of XPS, confirm that there is a depletion of rare earth elements, i.e. Pr on the sample surface after immersion. The detection of Pr related species on the pristine and corroded Mg–15 wt % Pr as-spun by XPS was probably due to its high content of Pr (15 wt %), in comparison with 5 wt % Nd in EA55RS extrusion. Nevertheless, the depletion of either Nd or Pr on the corroded samples in rare-earth containing Mg alloys is quite clear. The effect of this depletion on the surface on the corrosion resistance of rare-earth containing Mg alloys is still under investigation.

5. Conclusions

Surface characterization of the corrosion products formed on the surfaces and the original surfaces has been carried out for melt-spun Mg–Pr alloys immersed in 3% NaCl solution. $Mg(OH)_2$ and MgO were found on the pristine and corroded surfaces with $Mg(OH)_2$ as the predominant species after long times of immersion. A depletion of rare-earth Pr from the corroded sample surface was found by SIMS depth profiling.

References

1. D. RUGG, R. G. J. EDYVEAN and H. JONES, *Mater. Sci. Technol.* **9** (1993) 994.
2. S. K. DAS and C. F. CHANG, US Patent, 4765954, 23 August 1988.
3. *Idem.*, US Patent 4853035, August, 1989.
4. Y. LI and H. Y. LIU, *J. Mater. Process Technol.* **48** (1995) 483.
5. Y. LI, S. C. NG and C. H. KAM, unpublished results.
6. J. CHASTAIN (ed.), "Handbook of X-ray photoelectron spectroscopy" (Perkin-Elmer Corporation, Physical Electronics Division, Eden Prairie, MI, USA, 1990).
7. Y. LI, J. LIN, F. C. LOH, K. L. TAN and H. JONES, *J. Mater. Sci.* **31** (1996) 4017.
8. S. KRISHNAMURTHY, M. KHOBAIB, E. ROBERTSON and F. H. FROES, *Mater. Sci. Eng.* **99** (1988) 507.
9. C. B. BALIGA, P. TSAKIROPOULOS and J. F. WATTS, *Int. J. Rapid Solidif.* **4** (1989) 231.
10. C. B. BALIGA, P. TSAKIROPOULOS and C. JEYNES, *J. Mater. Sci.* **26** (1991) 1497.
11. C. B. BALIGA and P. TSAKIROPOULOS, *Mater. Sci. Eng. A.* **A134** (1991) 1029.
12. *Idem.*, *Mater. Sci. Technol.* **9** (1993) 507.
13. D. S. AHMED, R. G. J. EDYVEAN, C. M. SELLARS and H. JONES, *ibid.* **9** (1990) 469.
14. G. L. MAKER, J. KRUGER and K. SIERADZKI, *J. Electrochem. Soc.* **139** (1992) 47.